Parity violation in ^{232}Th neutron resonances above 250 eV

E. I. Sharapov,[1] J. D. Bowman,[2] B. E. Crawford,[3,*] P. P. J. Delheij,[4] C. M. Frankle,[2] M. Iinuma,[5,†] J. N. Knudson,[2] L. Y. Lowie,[6,‡] J. E. Lynch,[7] A. Masaike,[5,§] Y. Matsuda,[5,‖] G. E. Mitchell,[6] S. I. Penttilä,[2] H. Postma,[8,¶] N. R. Roberson,[3] S. J. Seestrom,[2] S. L. Stephenson,[6,*] Y.-F. Yen,[2,**] and V. W. Yuan[2]

[1]*Joint Institute for Nuclear Research, 141980 Dubna, Russia*

[2]*Los Alamos National Laboratory, Los Alamos, New Mexico 87545*

[3]*Duke University, Durham, North Carolina 27708*
and Triangle Universities Nuclear Laboratory, Durham, North Carolina 27708-0308

[4]*TRIUMF, Vancouver, British Columbia, Canada V6T 2A3*

[5]*Physics Department, Kyoto University, Kyoto 606-01, Japan*

[6]*North Carolina State University, Raleigh, North Carolina 27695-8202*
and Triangle Universities Nuclear Laboratory, Durham, North Carolina 27708-0308

[7]*Gettysburg College, Gettysburg, Pennsylvania 17325*

[8]*Delft University of Technology, Delft, 2600 GA, The Netherlands*

(Received 7 September 1999; published 18 January 2000)

The analysis of parity nonconservation (PNC) measurements performed on ^{232}Th by the TRIPLE Collaboration has been extended to include the neutron energy range of 250 to 1900 eV. Below 250 eV all ten statistically significant parity violations have the same sign. However, at higher energies PNC effects of both signs were observed in the transmission of longitudinally polarized neutrons through a thick thorium target. Although the limited experimental energy resolution precluded analysis in terms of the longitudinal asymmetry, parity violations were observed and the cross section differences for positive and negative neutron helicities were obtained. For comparison, a similar analysis was performed on the data below 250 eV, for which longitudinal asymmetries were obtained previously. For energies below 250 eV, the *p*-wave neutron strength functions for the $J=1/2$ and $J=3/2$ states were extracted: $S^1_{1/2}=(1.68\pm0.61)\times10^{-4}$ and $S^1_{3/2}=(0.75\pm0.18)\times10^{-4}$. The data provide constraints on the properties of local doorway states proposed to explain the PNC sign effect in thorium.

PACS number(s): 24.80.+y, 25.40.Ny, 27.90.+b, 11.30.Er

I. INTRODUCTION

The Time Reversal Invariance and Parity at Low Energy (TRIPLE) Collaboration discovered [1,2] an unexpected sign correlation in the longitudinal asymmetries of the ^{232}Th *p*-wave neutron cross sections measured with polarized neutrons. The longitudinal asymmetries, *p*, are defined by

$$\sigma^{\pm}(E)=\sigma_{\mathrm{p}}(E)(1\pm p), \tag{1}$$

where $\sigma^{\pm}(E)$ is the neutron cross section for the + and – neutron helicity states, and $\sigma_{\mathrm{p}}(E)$ is the *p*-wave resonance cross section for unpolarized neutrons. The cross section depends on the energy *E*, neutron width Γ_n, total width Γ, and resonance energy E_0, while the asymmetry *p* is constant for a given resonance with the value depending on the specific resonance parameters and the weak matrix elements between the compound states. The parity nonconservation (PNC) effects result from mixing (by the weak interaction) of compound states with different parity and the same spin. For ^{232}Th (a target with spin I = 0) *s*-wave neutrons excite states with spins $J=1/2$, while *p*-wave neutrons (orbital angular momentum $l=1$) excite compound states with spins $J=1/2$ and $J=3/2$. Parity violation may occur only in the $J=1/2$ resonances. Although there have been no direct measurements to determine the spins of the *p*-wave resonances in thorium, the PNC data serve to assign spin $J=1/2$ to those resonances that show parity violation.

The sign correlation effect in thorium was confirmed in a recent measurement [3] which shows ten statistically significant asymmetries below 250 eV, all with positive sign (the same as the sign of the PNC effect at 0.74 eV in ^{139}La). This is unexpected, since the longitudinal asymmetry is presumably [1,4] a mean zero Gaussian variable. Numerous theoretical attempts were made to explain this nonstatistical effect. The early attempts focused on distant doorway states; all failed because these explanations required a weak single particle matrix element at least two orders of magnitude larger than consistent with all other information. These efforts are summarized by Stephenson *et al.* [3]. More recent attempts to explain the sign correlation effect have invoked local doorways [5–8]. At present there is no generally accepted explanation for the sign effect. Many of the theoretical dis-

*Present address: Gettysburg College, Gettysburg, PA 17325.

†Present address: Hiroshima University, Hiroshima-Ken 739-8526, Japan.

‡Present address: McKinsey and Company, Atlanta, GA 30303.

§Present address: Fukui University of Technology, 3-6-1 Gakuen, Fukui-shi, 910-8505, Japan.

‖Present address: Institute of Physical and Chemical Research (RIKEN), Saitama, 351-0198, Japan.

¶Present address: IRI/ISO/TUD, 2629 JB Delft, The Netherlands.

**Present address: Wake Forest University School of Medicine, Winston-Salem, NC 27157.

 ©2000 The American Physical Society

cussions emphasize the need for PNC data at higher energies in thorium, in order to constrain the properties of the hypothetical doorways.

With the improved sensitivity of the TRIPLE experimental system, and extension of the measurement to higher energies, one might expect to observe PNC effects above the highest previously observed parity violating resonance at 232 eV. The standard analysis procedure to obtain the asymmetries p relies on knowledge of the resonance cross sections $\sigma_p(E)$. However, such an analysis is unreliable at higher energies since the limited experimental resolution obscures many p-wave resonances. Due to the large interest in the sign correlation effect, the TRIPLE Collaboration published the improved lower energy data [3] (where a complete analysis was possible), and decided to consider the remaining higher energy data separately. In Stephenson *et al.* [3] a cutoff energy of 285 eV was adopted—of course the choice of a specific cutoff energy is somewhat arbitrary. In the present paper the data above 250 eV are presented. These data are analyzed in terms of the PNC cross section differences $\Delta\sigma(E)=\sigma^+(E)-\sigma^-(E)$, instead of the asymmetries p.

II. PNC TRANSMISSION ASYMMETRIES: $\Delta\sigma$ EXTRACTION

In the present analysis it is important to distinguish between the (ideal) Breit-Wigner cross section difference $\Delta\sigma(E)$, the Doppler-broadened cross section difference $\Delta\sigma_D(E)$, and the resolution-broadened cross section difference $\Delta\sigma_R(E)$. The last quantity is related directly to the PNC transmission experiment, while the quantity $\Delta\sigma(E)$, which is convenient for theorists [9,10], must be determined indirectly from $\Delta\sigma_R(E)$. The experiment measures the PNC transmission asymmetry, ϵ, which is the relative difference in the detector yield due to the neutron spin flip. Since the asymmetry is small, $\epsilon(E)$ can be related (see, for example, Refs. [4,11]) to $\Delta\sigma_R(E)$ by

$$\epsilon(E)=\frac{Y_{nf}(E)-Y_{fl}(E)}{Y_{nf}(E)+Y_{fl}(E)}\cong-\frac{n}{2}f_n\Delta\sigma_R(E). \tag{2}$$

Here $Y_{nf}(E)$ and $Y_{fl}(E)$ are the detector yields for the nonflipped (NF) and flipped (fl) states of the spin flipper device, n is the number of nuclei per cm^2 in the target, and f_n is the neutron beam polarization at the entrance of the spin flipper. Changing the sign of f_n, while maintaining the same conditions for the spin flipper and the data acquisition system, provides a sensitive method to determine whether an observed effect is real or a statistical artifact—a true PNC effect will show a change in sign while an artifact will not. The key point is that Eq. (2) provides the tool to perform the analysis without knowledge of the resonance parameters. Although precise information on p cannot be obtained with this approach, one can estimate the size of p by using calculated values of the average peak cross sections. The essential point is that even if the p-wave resonances themselves are not observed, one can still under favorable circumstances observe PNC effects, and determine their sign and approximate magnitude.

For simplicity we shall consider only peak effects: all energy dependent quantities in Eq. (2) will be evaluated at the p-wave resonance energy $E=E_0$. The general convolution form for the cross section is

$$\sigma_R(E)=\int\sigma_D(E')R(E,E')dE', \tag{3}$$

where $R(E,E')$ is the instrumental response function (discussed below) and $\sigma_D(E')$ is the Doppler-broadened cross section (see Lynn [12]). The peak cross section can be rewritten as

$$\sigma_R(E_0)=\sigma_D(E_0)r_{DR}(E_0). \tag{4}$$

Conversely, if r_{DR} is known, the deconvoluted Doppler peak cross section is

$$\sigma_D(E_0)=r_{DR}^{-1}(E_0)\sigma_R(E_0). \tag{5}$$

In its turn, the deconvoluted Breit-Wigner peak cross section is

$$\sigma(E_0)=r_{\sigma D}^{-1}(E_0)\sigma_D(E_0). \tag{6}$$

Combining Eqs. (5) and (6) gives the basic equation for our analysis:

$$\sigma(E_0)=r_{\sigma D}^{-1}(E_0)r_{DR}^{-1}(E_0)\sigma_R(E_0). \tag{7}$$

In our case, the function $r_{DR}^{-1}(E_0)$ can be approximated (see discussion below) by

$$r_{DR}^{-1}(E_0)=0.6+0.02E_0(eV), \tag{8}$$

while the function $r_{\sigma D}^{-1}(E_0)$ is well known in an analytical form (see Lynn [12])

$$r_{\sigma D}^{-1}(E_0)=1/(\alpha\sqrt{\pi}\exp\alpha^2(1-\mathrm{erf}\,\alpha)),$$

with

$$\alpha=\Gamma/2\Delta_D(E_0), \tag{9}$$

where the square of the Doppler width is $\Delta_D^2=4E_0(kT_{\mathrm{eff}})/A$, with T_{eff} the effective temperature [13] and A the mass number.

III. EXPERIMENTAL METHOD

A. Apparatus

The measurements [3] were performed by the TRIPLE Collaboration at the spallation pulsed neutron source [14] of the Manuel Lujan, Jr. Neutron Scattering Center at the Los Alamos Neutron Science Center. A detailed up-to-date description of the experimental setup and the measurement procedure is provided in Refs. [3,15]. Here we note only a few key features of the PNC apparatus that are relevant for our analysis. The neutron beam was longitudinally polarized ($|f_n|\simeq 70\%$) by transmission through a polarized proton target developed by Penttilä *et al.* [16]. The proton polarization direction (and correspondingly the sign of f_n) relative to the

polarizing magnetic field was reversed every few days. The neutron spin direction was reversed every 10 s by an adiabatic spin flipper devised by Bowman, Penttilä and Tippens [17]. The ^{232}Th sample had $n=3.40\times10^{23}$ nuclei/cm^2. To reduce the Doppler resonance broadening, the sample was cooled to 77 K by a liquid-nitrogen chiller. The chiller was placed at the exit of the spin flipper. Neutrons transmitted through the sample were counted at 56.7 m by a large area ^{10}B-loaded liquid scintillation detector [18], using a digital-current mode signal processing circuit and the time-of-flight (TOF) technique. The Y_{nf} and $Y_{\rm fl}$ detector yields were accumulated by the acquisition system in 30-min ''runs'' and stored on a disk in nonflipped (nf) and flipped (fl) data areas each containing 8192 TOF channels of width 100 ns. Both data areas were in turn subdivided, into good (stable-beam) and bad (unstable-beam) areas. The sorting was achieved by monitoring the flux after each neutron burst and checking against the average flux 20 times per run. If the flux deviated by more than 8% from the average, the data were labeled ''bad.'' The entire run was discarded from the analysis if the data in bad areas were more than 50% of the total data. Runs with chiller malfunctions (when the target temperature was higher than 80 K) were rejected as well. Finally, for this analysis, 147 runs were selected and their good data areas were summed for subsequent analysis using Eq. (2).

B. Resolution function and the deconvolution procedure

A crucial aspect of our analysis is the use of the measured instrumental TOF response function $R(E,E')$ of our experimental system. The instrumental response depends upon the flight path length, the shape of the neutron pulse after the moderator, and the timing characteristics of the detector and electronics. This function has been studied in detail [15,19] and was implemented in the code FITXS [20], which was written specifically to obtain the asymmetries p from the TOF spectra. With this code we calculated transmission through our sample at different resonances with and without the $R(E,E')$ function. We used as input the Doppler-broadened total cross sections obtained from resonance parameters of the ENDF data file for ^{232}Th [21]. Figure 1 [22] presents the cross section in the energy region 210 to 310 eV. The p-wave resonances are extremely weak, and there are s-wave interference minima which provide high intensity transmission maxima in the detector yield. Such energy ''windows'' in the vicinity of s-wave resonances are optimal for finding nonzero ϵ—the background cross section is smaller and the dynamic enhancement factor [4] is large because the s- and p-wave resonances are close in energy. A thick sample helps to amplify the size of an isolated weak resonance in transmission, but the poor resolution makes the weak p-wave peaks almost invisible on the high level of the surrounding ''background.''

An example of the calculated transmission for a relatively strong p-wave resonance at 302.4 eV is shown in Fig. 2 both for the idealized case (with no interfering s-wave resonances and with perfect resolution) at the bottom and with a realistic resolution function at the top. This comparison was performed for a number of resonances that satisfied the condition $n\sigma_D(E_0)\leqslant 1.0$. From these data we obtained values of $r_{DR}^{-1}=\sigma_D(E_0)/\sigma_R(E_0)$ for a range of E_0. We found the linear function of Eq. (8) to be a good representation for r_{DR}^{-1} above $\sim$50 eV. Below the energy of $\sim$100 eV, the peak deconvolution begins to depend progressively on the p-wave resonance parameters. Above the energy of $\sim$100 eV, the instrumental width $(\Delta E)_R$ dominates over the Doppler width Δ_D, and therefore for p-wave resonances, which are experimentally observed, the ratio $\sigma_D(E_0)/\sigma_R(E_0)$ is practically independent of the resonance parameters. The linear dependence for r_{DR}^{-1} is expected then, since r_{DR}^{-1} behaves approximately as the ratio $(\Delta E)_R/\Delta_D$; in our case $(\Delta E)_R\simeq 0.24\times10^{-3}E\sqrt{E}$,

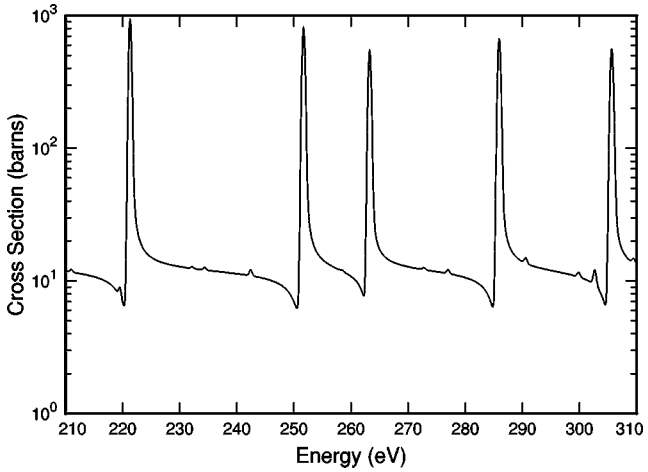

FIG. 1. The Doppler broadened total cross section calculated from the ENDF data, Ref. [21], for ^{232}Th in the energy range 210 to 310 eV. Plot produced by the T2 web server http://t2.lanl.gov/ using the program NJOY of MacFarlane *et al.*

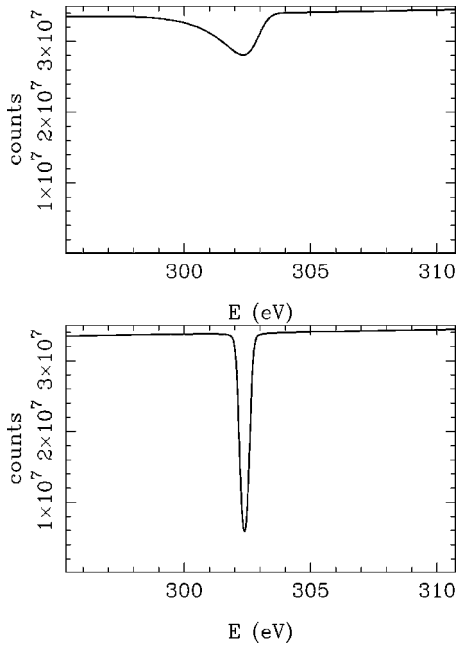

FIG. 2. Calculated transmission through the thorium sample due to the 302.4-eV p-wave resonance for perfect resolution (bottom) and with a realistic resolution function (top).

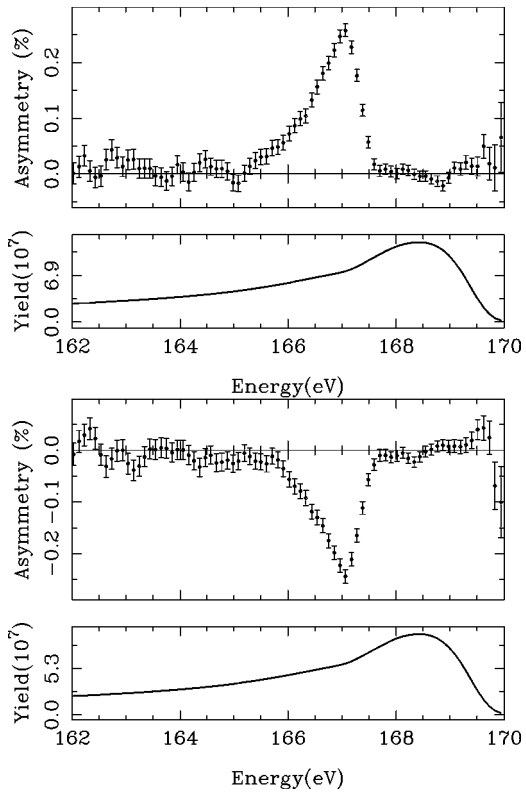

FIG. 3. Sample yield and transmission asymmetry ^{232}Th spectra near the 167.1-eV resonance for positive (top) and negative (bottom) polarizations of the proton target. The TOF scale is converted to the neutron energy scale. The yield is the sum $Y_{\mathrm{nF}}(E)+Y_{\mathrm{fl}}(E)$ and the asymmetry is defined by Eq. (2).

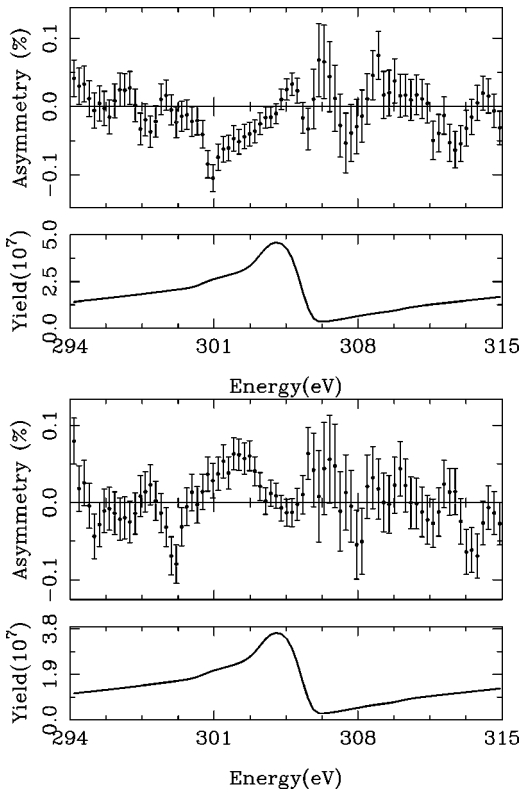

FIG. 4. Yield and transmission asymmetry ^{232}Th spectra near the 302.4-eV resonance for positive (top) and negative (bottom) polarizations of the proton target.

while $\Delta_D = 0.011\sqrt{E}$. Of course, the available TOF resolution sets the minimal value of the neutron width which can be observed at a given energy, e.g., $g\Gamma_n \sim 0.03$ meV [or $\sigma_p(E_0) \sim 10$ b] at 300 eV in our case.

There remains the question—under what conditions can this procedure for *cross sections* be applied to $\Delta\sigma_R(E)$ in Eq. (2). From the yield definition in Eq. (2) for an isolated *p*-wave resonance, it is clear that if the resonance transmission $\exp(-n\sigma_D)$ goes to zero (and therefore neutrons are not detected), then the $\Delta\sigma_D$ contribution to ϵ from the central region near $E=E_0$ will be suppressed in the instrumental convolution. To keep the systematic uncertainty of the deconvolution procedure below 10%, one should use a sample with $n\sigma_D(E_0) \leqslant 1.0$ for all *p*-wave resonances. In light of this requirement, our ^{232}Th sample ($n\sigma_s = 4.4$ for the potential scattering cross section $\sigma_s = 13.0$ b), was not optimal for the high energy study. We stress that the apparent suppression of the weak *p*-wave peaks on the large ''background'' count rate may not occur for the difference of the detector counts $Y_{\mathrm{nF}}(E) - Y_{\mathrm{fl}}(E)$. In a case of an ideal statistics, the count rate difference $Y_{\mathrm{nF}}(E) - Y_{\mathrm{fl}}(E)$ is expected to be large only near *p*-wave resonances that show a PNC effect.

IV. DATA AND RESULTS

A. PNC transmision asymmetry data

The neutron TOF yields and the PNC transmission asymmetries for selected energy regions are shown in Figs. 3–7. All of these figures show the background-unsubtracted spectra with the TOF-channel axis converted to the neutron energy scale. The 167.1-eV resonance shown in Fig. 3 is an example from our low energy data. The peak value of the asymmetry is quite large. The well-developed low energy tail of the transmission asymmetry is a characteristic feature of the TOF resolution function. The next example, Fig. 4, presents data near the 302.4-eV *p*-wave resonance. The transmission dip for this resonance is stronger than for the 167-eV resonance, and is situated near the interference maximum in the yield due to the *s*-wave resonance at 306 eV (note the strong dip on the right-hand side). However, the transmission asymmetries for the 167- and the 302.4-eV resonances are very different: the 302.4-eV resonance has a smaller asymmetry with a negative sign. Yield and transmission asymmetry ^{232}Th spectra near the 687-eV resonance are shown in Fig. 5. This resonance is on the interference yield maximum from the 688.0-eV *s*-wave resonance [21,24]. Aside from the three points on the tail, the asymmetric shape is typical of the TOF-resolution function for this energy region. This is a clear case of a new *p*-wave resonance. There is an additional small cusp that reverses sign just as a longitudinal asymmetry does. However, its width is too narrow to be a real PNC effect and therefore it is most likely to be an artifact. Yield and transmission asymmetry ^{232}Th spectra near 1517 eV are shown in Fig. 6. There is a known *p*-wave resonance at 1516.5 eV [21,24], that is situated at the interference yield maximum due to the 1519.6- and 1525-eV *s*-wave resonances, which are visible as one broad dip in the yield spec-

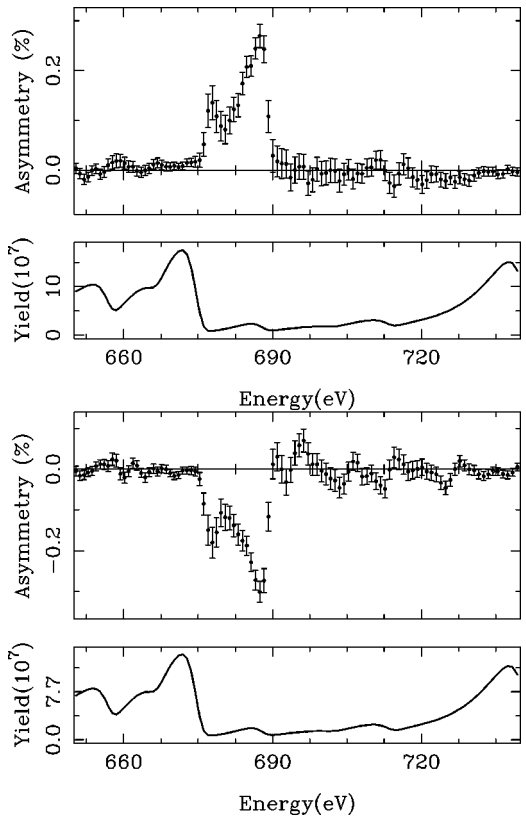

FIG. 5. Yield and transmission asymmetry ^{232}Th spectra near the 687-eV resonance for positive (top) and negative (bottom) polarizations of the proton target.

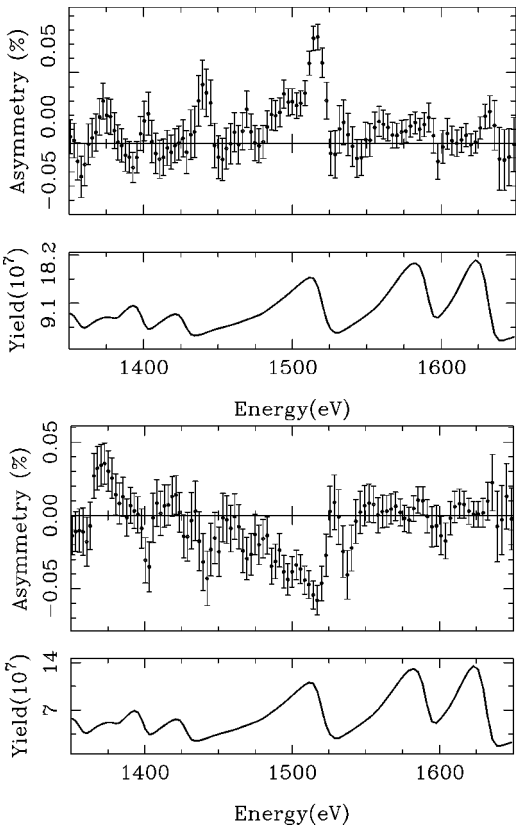

FIG. 6. Yield and transmission asymmetry ^{232}Th spectra near the 1517-eV resonance for positive (top) and negative (bottom) polarizations of the proton target.

tra. Finally, spectra in the energy region 1800–2100 eV are shown in Fig. 7. The asymmetries again occur at the interference maxima in the yield. The first effect corresponds to the known 1898.4-eV *p*-wave resonance [21,24], while the second effect corresponds to a new *p*-wave resonance.

B. Experimental results

The results for ϵ and $\Delta\sigma$ are listed in Table I together with $\Delta\sigma_p$ and σ_p calculated with Eq. (1) from the *p* values and resonance parameters reported in Refs. [3,21]. The results are presented only for resonances with an observed PNC effect. The resonance at 8.36 eV was not in the energy range of our data taken with 100-ns TOF width. Errors shown for ϵ and $\Delta\sigma$ are the statistical errors. The data in the fourth column stops at the last PNC effect reported in Ref. [3]. The last column in Table I lists the average peak resonance cross section $\langle\sigma_{p1/2}(E)\rangle$ calculated in the framework of the statistical model in two steps. First, the $J=1/2$ component of the energy averaged *p*-wave resonance cross section $\langle\sigma^1_{1/2}\rangle$ was obtained from

$$\langle\sigma^1_{1/2}(E)\rangle \cong 2\pi^2 R^2 \sqrt{E/(1\ \mathrm{eV})}\, S^1_{1/2}, \tag{10}$$

which is a good approximation to the exact expression [23] for our energy region. Here $R=1.35A^{1/3}$ fm is the neutron-nucleus interaction radius [24], E is the energy in eV, and $S^1_{1/2}$ is the *p*-wave neutron strength function for resonances with spins $J=1/2$. Next, the $p_{1/2}$ average peak resonance cross sections were calculated from $\langle\sigma_{p1/2}\rangle = 2\langle\sigma^1_{1/2}\rangle D_{p1/2}/(\pi\Gamma)$. We used the values $\Gamma=24.5$ meV, $D_{p1/2}=17$ eV (the same as the *s*-wave level spacing $D_{s1/2}$), and $S^1_{1/2}=1.68\pm0.61\times10^{-4}$. The latter value was obtained for energies below 285 eV, according to the definition $S^1_{1/2}=\langle\Gamma^1_{n1/2}\rangle/D_{p1/2}$, using the observed resonance parameters from Ref. [3], and the $J=1/2$ spin assignment for resonances with statistically significant PNC asymmetries. The other *p*-wave resonances have a smaller value of $S^1_{3/2}=(0.75\pm0.18)\times10^{-4}$ for the $J=3/2$ strength function. Comparison of $\Delta\sigma$ with $\Delta\sigma_p$ for resonances below 250 eV shows that the two analysis methods agree for all but the two resonances at 128.17 and 196.20 eV. For these resonances the new values are approximately a factor of 2 smaller. Comparing the peak cross sections σ_p with the expected averaged values σ_{av}, we note that these two resonances are the strongest *p*-wave resonances, and as discussed above, suppression of the $\Delta\sigma$ contribution is expected. The observed resonance peak cross sections fluctuate because they are proportional to the neutron widths, which obey the very broad Porter-Thomas distribution. Therefore, we underestimate $\Delta\sigma$ by a factor of 2 for resonances which are several times stronger than the average value at the corresponding energy.

C. Matrix elements

For several reasons we believe that the newly observed asymmetries ϵ are true PNC effects. The values of $\epsilon(E$

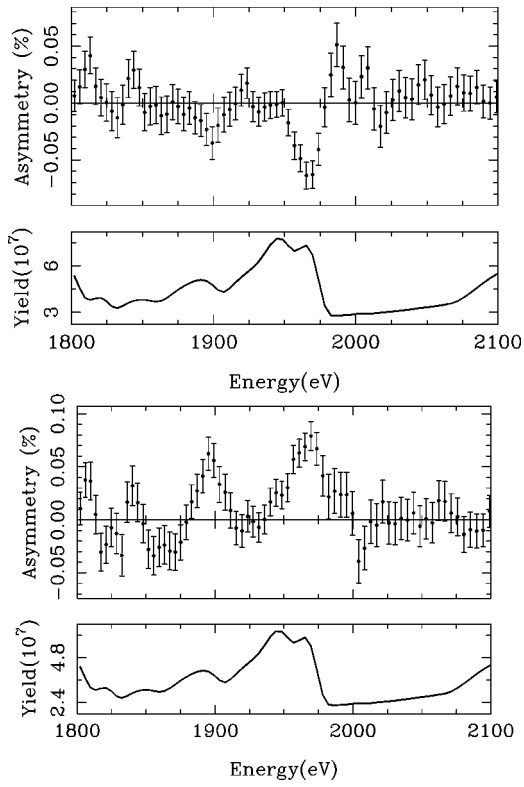

FIG. 7. Yield and transmission asymmetry ^{232}Th spectra near the 1898-eV and 1967-eV resonances for positive (top) and negative (bottom) polarizations of the proton target.

$=E_0$) are statistically significant. The fact that $\epsilon(E=E_0)$ changes sign for positive and negative proton polarizations is a very strong argument in favor of the effects being true PNC effects and not statistical accidents. The cases at the 302.4, 1517, and 1898 eV correspond to known *p*-wave resonances at 302.6, 1516.6, and 1898.4 eV, respectively [21,24]. Although only the 302.4-eV resonance is observed in the summed TOF spectrum $Y_{nf}+Y_{\mathrm{fl}}$ because of the high count level in the vicinity and the poor resolution, the new resonances are observed in the yield difference $Y_{nf}-Y_{\mathrm{fl}}$ due to their apparent PNC effect.

In order to consider whether the new $\Delta\sigma$ values are consistent with our lower energy data in thorium, we determined the weak matrix elements θ using the two-level approximation. The *s*-wave resonance (at energy E_s) that is closest to the PNC effect was assumed to be responsible for the entire effect. Using Eq. (1) and the widely used expression $p=2\theta\sqrt{\Gamma_n^s/\Gamma_n^p}/(E_s-E_0)$ [4], we obtain

$$\Delta\sigma(E=E_0)=16\pi R^2\theta\sqrt{\Gamma_n^0\Gamma_n^1}/[k_1R(E_s-E_0)\Gamma], \quad (11)$$

where Γ_n^0 and Γ_n^1 are the reduced neutron widths of the *s*- and *p*-wave resonances, k_1 the neutron wave number at $E=1$ eV, Γ the total width of the *p*-wave resonance, and θ the weak matrix element. For the new *p*-wave resonances, for which there are no measured widths, we estimated Γ_n^1 from the corresponding average peak cross section given in Table I. The results for individual matrix elements θ are 0.15, 0.35, 2.0, 1.8, 1.7, and 8 meV for the resonances at 250, 302.4, 687, 1517, 1898, and 1967 eV, respectively. The same procedure applied to resonances below 250 eV gave individual matrix elements in the range 0.5 to 5.0 meV, with an average

TABLE I. Longitudinal transmission asymmetries ϵ, PNC cross section differences $\Delta\sigma$, and resonance cross sections for ^{232}Th.

E_0 (eV)	ϵ (10^{-3})	$\Delta\sigma$ (mb)	$\Delta\sigma_p$ (mb)[a]	σ_p (b)[a]	$\langle\sigma_{p1/2}\rangle$ (b)[b]
8.36[c]			121±6	3.39	2.9
38.23	3.50±0.25	156±11	172±19	1.34	6.2
47.07	3.30±0.20	180±11	197±15	3.92	6.9
64.57	4.41±0.18	332±13	368±25	1.30	8.0
98.06	0.54±0.16	67±20	65±20	4.64	9.9
128.17	6.32±0.35	1210±68	3063±260	66.3	11.3
167.11	2.37±0.09	581±22	957±105	14.9	13.0
196.20	0.90±0.27	265±80	682±150	37.9	14.0
202.58	0.95±0.15	310±50	486±130	22.1	14.2
231.95	1.30±0.13	470±50	445±89	4.66	15.3
250.0	−0.27±0.05	−110±20		–	15.8
302.4	−0.58±0.06	−320±33		49[d]	17.4
687.2	3.00±0.10	5250±180			26.3
1517	0.70±0.04	3650±210		115[d]	39.0
1898	−0.50±0.13	−3600±900		213[d]	43.6
1967	−0.80±0.08	−6310±630			44.4

[a]Calculated from data of Ref. [3].
[b]Calculated with the use of $S_{1/2}^1$.
[c]Not analyzed in this work.
[d]Calculated from data of Ref. [21].

value of 1.8 meV. The detailed likelihood analysis of the set of longitudinal asymmetries $\{p\}_E$ for resonances below 250 eV gave the value of the root-mean-square matrix element of $(1.58^{+0.44}_{-0.31})$ meV [3]. Therefore the $\Delta\sigma$ values for the six new PNC effects in ^{232}Th are completely consistent with those obtained from the PNC effects at lower energy in ^{232}Th.

V. CONCLUSION

In summary, we again emphasize that the experimental conditions for these measurements (the flight path, detector, and sample thickness) were not optimized for the neutron energy region that we have analyzed here. In particular, the energy resolution was poor. The energy regions that are sensitive to the observation of PNC effects are very limited—only those regions near the *s*-wave interference cross section minima. In those regions we observed four negative and two positive statistically significant longitudinal transmission asymmetries. Three of these correspond to known resonances and three others to new *p*-wave resonances in ^{232}Th. The longitudinal transmission asymmetries ϵ were converted to PNC differences of the *p*-wave resonance peak cross sections $\Delta\sigma$. The systematic uncertainty due to this conversion is about 15% for those resonances whose strength is less than or equal to the average strength in ^{232}Th. For stronger resonances, the $\Delta\sigma$ value could be as much as twice as large. The size of the PNC asymmetries observed at high energies can be estimated with the use of average *p*-wave peak cross sections. The asymmetry values do not exceed 10%, consistent with the values observed at energies below 250 eV [3]. The individual weak matrix elements for the new effects were estimated in the two-level approximation. They are consistent with the rms matrix element determined from detailed analysis of the lower energy data.

The new results show that negative PNC effects in ^{232}Th appear at neutron energies above 250 eV. This provides some constraints on the properties of doorway states proposed to explain the PNC sign effect in thorium. Due to the selectivity of these measurements—only for large PNC effects and only in the *s*-wave interference regions—these results do not represent a complete picture of PNC effects in ^{232}Th at higher energies. Any detailed inference regarding the behavior of the PNC effects in ^{232}Th seems premature without dedicated measurements with neutrons above 250 eV.

ACKNOWLEDGMENTS

This work was supported in part by the U.S. Department of Energy, Office of High Energy and Nuclear Physics, under Grants No. DE-FG02-97-ER41042 and DE-FG02-97-ER41033. The work was performed at the Los Alamos Neutron Science Center at the Los Alamos National Laboratory. This facility is funded by the U.S. Department of Energy, Office of Energy Research, under Contract No. W-7405-ENG-36.

[1] C. M. Frankle *et al.*, Phys. Rev. Lett. **67**, 564 (1991).
[2] C. M. Frankle *et al.*, Phys. Rev. C **46**, 778 (1992).
[3] S. L. Stephenson *et al.*, Phys. Rev. C **58**, 1236 (1998).
[4] O. P Sushkov and V. V. Flambaum, JETP Lett. **32**, 352 (1980).
[5] B. Desplanques and S. Noguera, Nucl. Phys. **A598**, 139 (1996).
[6] N. Auerbach, J. D. Bowman, and V. Spevak, Phys. Rev. Lett. **74**, 2638 (1995).
[7] V. V. Flambaum and V. G. Zelevinsky, Phys. Lett. **94B**, 277 (1995).
[8] M. S. Hussein, A. K. Kerman, and C.-Y. Lin, Z. Phys. A **351**, 30 (1995).
[9] S. E. Koonin, C. W. Johnson, and P. Vogel, Phys. Rev. Lett. **69**, 1163 (1992).
[10] B. V. Carlson, M. S. Hussein, A. K. Kerman, and C.-Y. Lin, Phys. Rev. C **52**, R11 (1995).
[11] V. P. Alfimenkov, S. B. Borzakov, Vo Van Thuan, Yu. D. Mareev, L. B. Pikelner, A. S. Khrykin, and E. I. Sharapov, Nucl. Phys. **A398**, 93 (1983).
[12] J. E. Lynn, Nucl. Instrum. Methods **9**, 315 (1960).
[13] W. E. Lamb, Phys. Rev. **55**, 190 (1939).
[14] P. W. Lisowski, C. D. Bowman, G. J. Russell, and S. A. Wender, Nucl. Sci. Eng. **106**, 208 (1990).
[15] B. E. Crawford *et al.*, Phys. Rev. C **58**, 1225 (1998).
[16] S. I. Penttilä, J. D. Bowman, P. P. J. Delheij, C. M. Frankle, D. G. Haase, H. Postma, S. J. Seestrom, and Yi-Fen Yen, in *High Energy Spin Physics*, edited by K. J. Heller and S. L. Smith (American Institute of Physics, New York, 1995), p. 532.
[17] J. D. Bowman, S. I. Penttilä, and W. B. Tippens, Nucl. Instrum. Methods Phys. Res. A **369**, 195 (1996).
[18] Yi-Fen Yen *et al.*, Nucl. Instrum. Methods Phys. Res. A (to be published).
[19] B. E. Crawford, Ph.D. dissertation, Department of Physics, Duke University, 1997.
[20] J. D. Bowman, Y. Matsuda, B. E. Crawford, and Y.-F. Yen, Program FITXS, 1997 (unpublished).
[21] D. K. Olsen, Report No. ORNL/TM-8056, 1982, ENDF-319, Oak Ridge National Laboratory.
[22] Plot produced by the T2 web server http://t2.lanl.gov/ using the program NJOY of R. E. MacFarlane *et al.*
[23] J. E. Lynn, *The Theory of Neutron Resonance Reactions* (Clarendon, Oxford, 1968).
[24] S. F. Mughabghab, M. Divadeenam, and N. E Holden, *Neutron Cross Sections* (Academic Press, New York, 1984) Vol. 1, Pt. B.